Investigation on Laser Material Processing of Glass by Simultaneous Short and Ultrashort Pulses

Sebastian Funken*[1], Jiri Martan[2], and Harald Riegel[1]

[1]*Aalen University, LaserApplicationCenter, 73430 Aalen, Germany*
[2]*University of West Bohemia, New Research Technologies Centre (NTC), 30100 Plzen, Czech Republic*
**Corresponding author's e-mail: sebastian.funken@hs-aalen.de*

Processing heat-sensitive materials like glass requires minimizing thermal damage, a challenge for conventional nanosecond lasers. While ultrashort pulsed lasers offer precision, their efficiency can be limited. This study presents method to enhance glass processing by using a mixed-pulse-train (MPT) of synchronized picosecond (ps) and nanosecond (ns) pulses. We demonstrate that this simultaneous approach significantly improves ablation efficiency on soda-lime glass by determining the influence of the nanosecond pulse on the ablation threshold. The ablation threshold was reduced from 3.38 J/cm^2 with ps-only pulses to 2.79 J/cm^2 in MPT mode. This enhancement is critically dependent on the temporal delay, with the lowest threshold achieved when the ns pulse trails the ps pulse by 5 ns. This indicates a synergistic effect where the ps pulse pre-excites the material, increasing the absorption of the following ns pulse. Furthermore, MPT processing resulted in distinct topographical changes, including a wider modification zone and surface elevations up to 40 nm, suggesting localized volume expansion. These findings show that synchronized ps-ns pulses provide a highly controllable method for tailoring material interactions, offering a promising alternative to more complex and costly burst-mode systems for high-precision applications.
DOI: 10.2961/ilmn.2026.01.2009
Keywords: simultaneous pulses, mixed-pulse-train, nanosecond pulses, ultrashort pulses, ablation, soda-lime, glass

1. Introduction

Short and ultrashort pulsed lasers have become essential tools in industrial applications such as consumer electronics, micro-manufacturing, and medical engineering—especially for the precision processing of transparent materials like glass. Their ability to deliver highly localized energy through non-linear absorption mechanisms allows for micrometer-scale resolution and minimal heat-affected zones, making them particularly suitable for applications such as waveguide writing, microfluidics, and surface texturing [1,2]. Lasers operating in the nanosecond (ns) regime are valued for their relatively high average powers and fast processing speeds. However, their low peak intensity often limits their applicability in transparent dielectrics, where linear absorption is insufficient. As a result, achieving ablation typically requires higher pulse energies, which in turn introduces unwanted thermal effects such as melting, cracking, or delamination [3]. In contrast, ultrashort pulses in the picosecond (ps) and femtosecond (fs) regimes enable energy deposition via non-linear mechanisms like multiphoton ionization, making them highly effective for precise, high-quality structuring of glass with minimal damage [4,5]. Despite their advantages in terms of quality, their lower energy-per-pulse and limited throughput have motivated efforts to improve efficiency without compromising precision.

A promising strategy to bridge this gap lies in temporal pulse shaping and multi-pulse processing schemes, such as double-pulse and burst-mode operation. By combining pulses of different durations or subdividing a single laser pulse into a train of closely spaced sub-pulses, new interaction regimes can be accessed that offer enhanced control over material removal and modification. Laser processing with ultrashort double pulses has garnered increasing attention since the early 2000s. More recently, burst processing, in which a single pulse is divided into multiple sub-pulses with delays in the range of several hundred femtoseconds to a few microseconds, has demonstrated significant potential in the micromachining [6,7]. These bursts have been shown to improve ablation efficiency, surface quality, and structuring rates by leveraging physical effects such as transient plasma dynamics, re-deposition shielding, and melt layer manipulation. In this context, we investigate a simultaneous pulse approach based on a dual-seed laser system capable of emitting synchronized sub-ps- and ns-pulses at 1030 nm with tuneable delay. This configuration allows us to explore the interplay between an ultrashort preconditioning pulse and a trailing longer pulse in soda-lime glass. The objective of this work is to establish an understanding of the material response in glass under the combined ps-/ns-pulse irradiation. This understanding is critical for developing new fabrication strategies for surface as well as internal material modification, particularly for applications like optical waveguide writing, where both structural quality and process scalability are critical. [8-10]

2. Methods and Materials

For the laser processing in this study, a VaryDisk laser system (Dausinger+Giesen GmbH, Stuttgart, Germany) was utilized. This system generates 1030 nm pulses with an adjustable repetition rate up to 200 kHz. It supports two distinct pulse duration ranges: ultrashort pulses (0.6–2 ps) and short pulses (5–12 ns), delivering a maximum average power of 100 W. Both pulse types are generated from their own seed lasers and are amplified within a shared amplifier. They can be emitted either separately or simultaneously as a Mixed Pulse Train (MPT) through the same beam path and exit window. In MPT mode, individual ns or ps pulses each carry 50% of the total pulse energy, capped by a system limit of 500 µJ total pulse energy. Furthermore, MPT mode allows for precise temporal control, enabling the ps pulse to be delayed relative to the ns pulse. An adjustable delay range of -5 to 5 ns can be set. A negative delay means the ps pulse arrives after or inside the ns pulse, while a positive delay indicates the ps pulse arrives before the ns pulse (Figure 1). A delay of 0 ns signifies the simultaneous emission of both pulses.

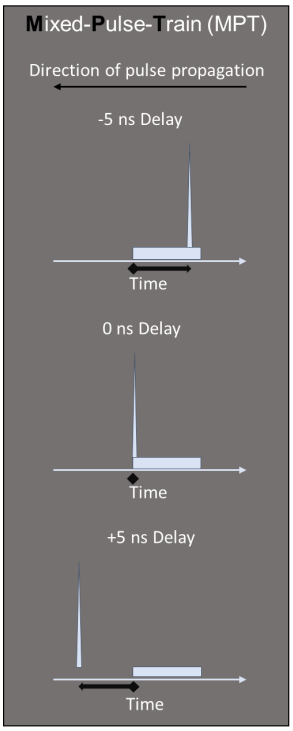

Fig. 1 Mixed-Pulse-Train: Simultaneous ns-ps pulses with possible delay-options between -5 and 5 ns. Example shown with a 2 ps and 5.5 ns pulse.

In addition to the NIR wavelength, green and UV can be converted using the integrated SHG and THG module. The laser source was integrated onto a "microcut UKP" USP machining system from LLT GmbH (Ilmenau, Germany). In the setup (Figure 2), the laser beam is focused onto the glass samples by an excelliSCAN14 galvo scanner system from SCANlab (Puchheim, Germany) in combination with a 100 mm telecentric F-theta lens from JENOPTIK Optical Systems GmbH (Jena, Germany). Achieving a focus diameter of approximately 32 µm and a Rayleigh length of 600 µm. The glass samples used in this study, which consisted of standard soda-lime glass microscope slides, were placed on the machine's precision table using a custom-made sample holder.

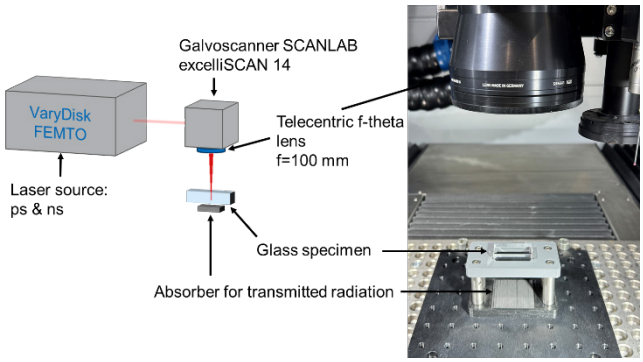

Fig. 2 Experimental setup.

The analysis of the surface structure after laser processing was performed with optical topography measurements using a Zygo NewView 8300 white light interferometer (WLI) and a Keyence VK-X3050 3D laser scanning confocal microscope (LSM).

3. Results and Discussion

The difference between ps-pulses and MPT is examined in more detail below. No results will be found for experiments with pure ns-pulses, as it was found that no ablation was visible under the selected parameters. Only uncontrollable cracking occurred at very high pulse energies.

First, the ablation behaviour of the different modes, ps-only and MPT pulse with delay -5 ns, 0 ns and 5 ns were investigated as single-pulse ablation. For this purpose, a frequency of 200 kHz was used with a high scanning speed to separate the pulses. The ablation threshold was then determined using the squared ablation diameter D_{th}^2 and the pulse energy E_P in logarithmic representation [11 12]. The pulse durations used in all experiments were 5.5 ns and 0.6 ps. The ablation threshold for pure ps pulses was determined to be 3.38 J/cm², comparable to the literature (Figure 3) [13].

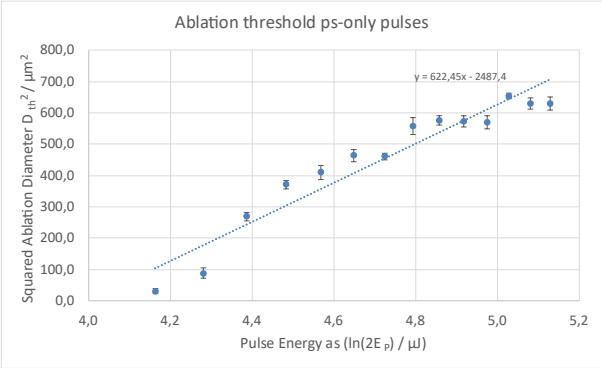

Fig. 3 Calculation of the Ablation threshold by [11] based on Liu [12] with 3.38 J/cm².

In MPT mode, the ablation threshold was determined solely based on the ps pulse energy. This approach allows to specifically evaluate how the simultaneous ns pulse influences the ps pulse's ablation characteristics. A reduction in this ps-pulse-based threshold, when compared to a pure ps-only process, directly indicates an energetic contribution from the ns pulse, effectively increasing the process's ablation efficiency. Figure 4 shows such a decrease in the

threshold for all MPT delay modes, confirming the partial interaction of the ns pulse that contributes to ablation. A closer look at the results under the individual MPT modes reveals that there are different degrees of coupling of the ns pulse depending on the delay time of the ps pulse. The delay of -5 ns shows a slightly higher ablation threshold with (3.14 J/cm²) than the 0 ns with (2.91 J/cm²) or 5 ns delay with (2.79 J/cm²).

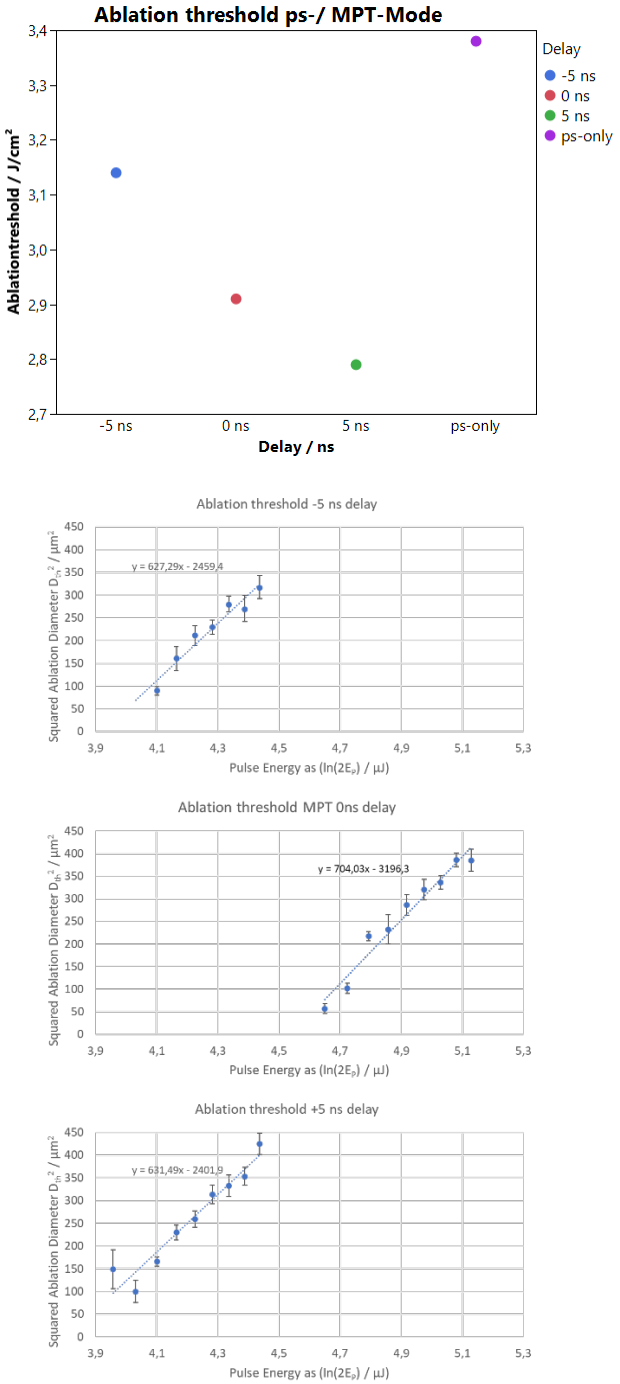

Fig. 4 Ablation threshold compared between pure ps and MPT pulses. In addition, the individual diagrams for determining the ablation threshold are shown here.

In the investigated configuration with a -5 ns delay, the picosecond (ps) pulse temporally overlaps with the longer nanosecond (ns) pulse, arriving during its envelope. This represents an overlapping interaction regime. The ps pulse initiates the ablation via non-linear absorption, creating an absorptive state while the ns pulse is already delivering energy. This results in a complex, simultaneous interaction where the ns pulse's role is to enhance or modify the effects established by the ps pulse, rather than acting as an independent driver. The different ablation threshold observed for this delay suggests a difference in the coupling efficiency of this mechanism compared to the sequential interaction of the +5 ns delay. This general approach of using a timed sequence to manage the material's electronic state draws conceptual parallels to the "shielding-free" ablation seen in high-frequency GHz burst modes [14]. It can be assumed that parts of the ns pulse are not coupled in due to plasma formation and that the overall absorption efficiency of the ns pulse suffers depending on the temporal synchronization to the ps pulse.

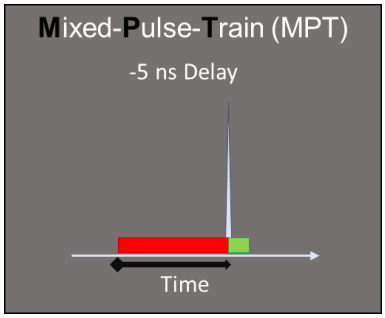

Fig. 5 Energy absorption regarding the MPT -5 ns delay ns pulse. The pulse durations 2 ps and 5.5 ns were used.

The other two modes show a further reduction in the ablation threshold. With a delay of 0 ns, both pulses hit simultaneously, which means that more energy is available from the ns pulse. A delay of 5 ns even shows that the subsequent ns pulse can couple even better. As also shown in the work of Zhang [15], the ablation efficiency increases while combining femtosecond and microsecond lasers. This efficiency is critically dependent on the temporal delay, which appears to define two distinct interaction regimes. In the case of the +5 ns delay, the interaction can be viewed as a sequential, two-stage process. First, the high peak intensity of the ps pulse induces a transient electron excitation, lifting electrons from the valence band to the conduction band and momentarily giving the glass metallic, absorptive properties [16]. The trailing ns pulse then efficiently deposits its energy into this pre-conditioned state, likely heating the free carriers through inverse bremsstrahlung and enhancing material removal.

In addition to the reduction of the ablation threshold due to the partial absorption of the ns pulse, there are other effects that are clearly visible when processing lines. In the following, experiments were carried out on the ablation of lines with a pulse overlap of 80 %.

Initially, ablation was also considered using only the ps pulses. This shows an inconspicuous ablation line (Figure 6) with some particle emission and a small heat-affected zone directly around the ablation. For the topology, only the area

around the ablation was considered, the ablated region is masked. While a detailed analysis of the ablation depth and material removal rate would be critical for optimizing surface machining applications, the focus of this work was to establish the fundamental influence of the ns pulse on the energy coupling and material modification, providing a basis for future studies on internal structuring of transparent materials. In Figure 6 a small influence zone of about ~19.5 µm in width can be seen for the ps pulse, in which there appears to be an elevation of the surface < 20 nm. This may indicate a modification of the glass around the ablation.

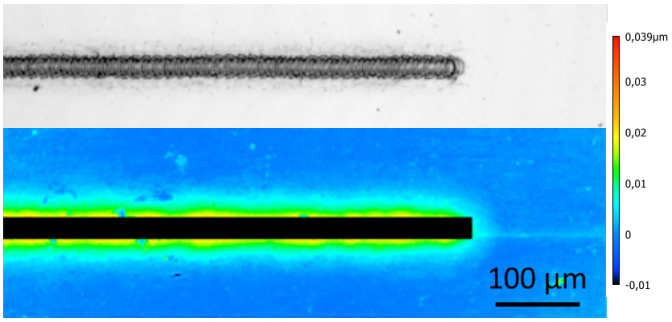

Fig. 6 WLI measurement of ps-only ablation 42 µJ pulse energy (5.22 J/cm²). On top is the microscopic image of the ablated region. On the bottom is the surface topography image, where a narrow elevation due to modification can be seen. The ablated region is masked to highlight the structure of the modification.

For the MPT modes, a clear difference can already be seen in the microscope image (Figure 7), here the area directly around the ablation site appears clearly altered with frayed edges. This change has an extent of about 19 µm, but was not visible in this form in the pure ps. The topology image (Figure 7) also shows a clearly different picture, with a much larger influence zone of around ~61.8 µm. Overall, there is a stronger modification of the glass, as can be seen from the stronger elevation of the glass with around 20-40 nm in height. The MPT modes, especially the extreme cases of -5 and 5 ns, do not differ from each other in terms of topology and both show a clear modification of the surrounding glass.

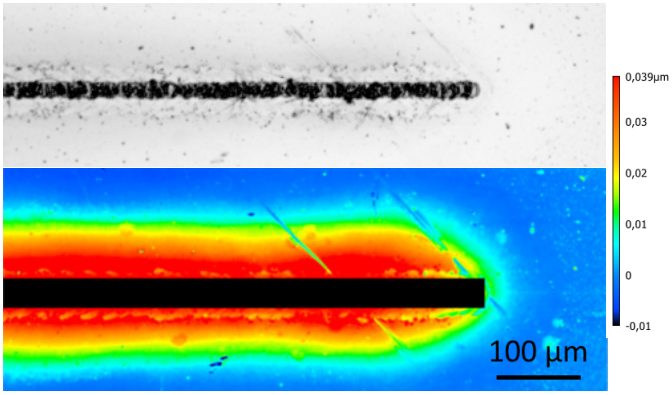

Fig. 7 WLI measurement of MPT ablation (-5 ns delay) 84 µJ combined pulse energy (10.45 J/cm² combined Fluence, ps: 5.225 J/cm² and ns: 5.225 J/cm²). On top is the ablated microscopic image. On the bottom is the surface topography image, where a wide elevation due to modification can be seen. The ablated region is masked to highlight the structure of the modification.

A structural modification caused by laser processing, which is accompanied by a local reduction in density and a resulting volume expansion, seems plausible. Figure 8 illustrates the mechanism of laser-induced structural modification in glass. The intense, ultrashort laser pulse deposits energy via non-linear absorption, which is sufficient to break the Si-O bonds within the glass network. This allows the atomic structure to reorganize upon cooling. The network resettles into a configuration with larger, more open ring structures, a state that is less dense than the original material. [17] The arrows in the sketch represent the consequence of this structural change: volume expansion. As the glass network reorganizes into a less dense state, it occupies more volume, creating internal stress that pushes outward against the surrounding, unmodified material. Because the material cannot expand well into the unmodified material, the modification can be measured as a raised area on the surface. If the modification were deeper, this would not be the case, as stress would be introduced into the material. This localized expansion is what manifests as the nanometer-scale surface elevation observed in the WLI measurements. This expansion typically manifests itself on the sample surface in the form of an elevation in the nanometer range. Corresponding phenomena have already been observed in earlier studies for this type of glass. It was shown that the extent of the volume change depends significantly on the specific glass type and manufacturing process, which points to material-dependent mechanisms of structural reorganization [18].

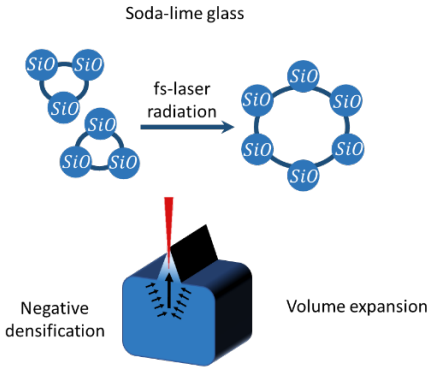

Fig. 8 Volume expansion due to change in density regarding soda-lime glass. The small arrows represent the interface of modified and unmodified material resulting in the directed volume expansion (big arrow).

4. Conclusion

In this study, we investigated the interaction of combined ultrashort and short laser pulses in the context of laser material processing of soda-lime glass using a mixed pulse train configuration. The results clearly demonstrate that the temporal synchronization of the two pulse types play a decisive role in both the initiation and the extent of laser-induced modifications. Pure nanosecond pulses, under the applied conditions, did not lead to controlled ablation but instead caused uncontrollable cracking at high pulse energies, confirming their limited applicability as a standalone tool for precision micro structuring of glass.

The introduction of MPT configurations, where ps and ns pulses are temporally synchronized with programmable delays, revealed a significant reduction in the ablation threshold compared to the ps-only case. This reduction confirms a synergistic interaction in which the ps pulse initiates the material excitation through non-linear absorption processes, enabling partial absorption of the trailing ns pulse. The experimental data show that the ablation threshold depends on the temporal delay between the two pulses: the lowest threshold was observed at a delay of +5 ns, while a slight increase was measured at a -5 ns delay. These findings are in line with previously reported studies indicating that nanosecond pulses can more effectively deposit energy into pre-excited material states, such as transient electron excitation or plasma-modified regions, provided a suitable delay is introduced between the pulse pairs.

Beyond the threshold behaviour, differences in topography and surface modification were evident when comparing line ablations with and without MPT. While ps-only processing yielded narrow, sharply defined structures with minimal peripheral modification, the MPT modes led to substantially wider zones of influence. The surface elevations observed in the nanometer range (up to ~40 nm) strongly suggest structural reorganization within the glass, likely involving a localized density reduction and corresponding volume expansion. These effects were consistently observed for both -5 ns and +5 ns MPT delays and align well with literature reports of laser-induced glass modification.

Taken together, these results underscore the importance of pulse timing and sequence in simultaneous laser processing strategies. The MPT configuration, particularly with optimized temporal delays, provides a promising approach to enhance ablation efficiency and to tailor structural modifications in transparent materials. Building on this, future investigations will focus on systematically varying the pulse duration combinations. The ability to fine-tune the degree of material interaction through temporal control offers new opportunities for the fabrication of micro- and nanoscale features in glass-based devices, with potential relevance to integrated photonics, microfluidics, and biosensor applications. One particularly promising application lies in the inscription of optical waveguides in transparent materials. By optimizing the temporal sequence and energy balance of the pulses, it may be possible to induce smooth, symmetric index profiles and to tailor the guiding properties.

Acknowledgments and Appendixes

The authors acknowledge support by the German Federal Ministry of Education and Research (BMBF), Program 'FH-Kooperativ' (ProCEVen, grant no. 13FH135KX0).

References

[1] K. Sugioka and Y. Cheng: Light Sci. Appl., 3, (2014) e149.
[2] R. Osellame, G. Cerullo, and R. Ramponi: “Femtosecond Laser Micromachining: Photonic and Microfluidic Devices in Transparent Materials” ed. by C.E. Ascheron and A.H. Duhm (Springer, Berlin, 2012) p.444.
[3] A. C. Tam: Rev. Mod. Phys., 58, (1986) 381.
[4] B. C. Stuart, M. D. Feit, A. M. Rubenchik, B. W. Shore, and M. D. Perry: Phys. Rev. Lett., 74, (1995) 2248.
[5] C. B. Schaffer, A. Brodeur, J. F. Garcia, and E. Mazur: Opt. Lett., 26, (2001) 93.
[6] P. Lickschat, R. Heise, and M. Eberstein: Opt. Express, 22, (2014) 18177.
[7] R. Weber, T. Graf, M. Lenzner, T. Radel, and M. Weikert: Phys. Procedia, 83, (2016) 100.
[8] B. Neuenschwander, B. Jaeggi, M. Schmid, and U. Hunziker: Phys. Procedia, 39, (2012) 586.
[9] A. C. Tien, S. Backus, H. C. Kapteyn, M. M. Murnane, and G. Mourou: Phys. Rev. Lett., 82, (1999) 3883.
[10] N. Sanner, M. Siebold, E. Beyer, and M. Eberstein: Appl. Phys. A, 120, (2015) 1121.
[11] A. Feuer, C. Kunz, M. Kraus, V. Onuseit, R. Weber, T. Graf, und D. Ingildeev: Proc. SPIE 8967 (2014) 89670H
[12] J. M. Liu, Opt. Lett., 7, (1982) 196.
[13] D. Nieto, J. Arines, G. M. O’Connor, and M. T. Flores-Arias: Appl. Opt., 54, (2015) 8596.
[14] G. Bonamis, E. Audouard, C. Hönninger, K. Mishchik, I. Manek-Hönninger and J. Lopez, Opt. Express, 28, (2020) 23620.
[15] Y. Zhang, Y. Ito, R. Yoshizaki, A. Shibata, I. Nagasawa, K. Nagato, and N. Sugita, Opt. Express, 31, (2023) 38191.
[16] N. Miyamoto, Y. Ito, C. Wei, R. Yoshizaki, A. Shibata, I. Nagasawa, K. Nagato, and N. Sugita, Opt. Lett., 45, (2020) 3171.
[17] J. W. Chan, T. R. Huser, S. H. Risbud and D. M. Krol, Opt. Lett., 26, (2001) 1726.
[18] K. Miura, H. Inouye, S. Hirao, Appl. Phys. Lett., 71, (1997) 332.

(Received: June 13, 2025, Accepted: December 29, 2025)